

## Nucleophilic or Electrophilic Phosphinidene Complexes $ML_n=PH$ ; What Makes the Difference?

Andreas W. Ehlers, Evert Jan Baerends, and Koop Lammertsma\*

Contribution from the Department of Chemistry, Faculty of Sciences, Vrije Universiteit, De Boelelaan 1083, NL-1081 HV Amsterdam, The Netherlands

Received November 1, 2001

**Abstract:** Density functional studies, based on the local density approximation including nonlocal corrections for correlation and exchange self-consistently, have been carried out for the equilibrium structures of the phosphinidene transition metal complexes  $ML_n=PH$ , with  $M = Ti, Zr, Hf, V, Nb, Ta, Cr, Mo, W, Fe, Ru, Os, Co, Rh, Ir$  and  $L = CO, PH_3, Cp$ . The chemical reactivity of the transition metal-stabilized phosphinidene  $P-R$  is influenced by its spectator ligands  $L$ . Ligands with strong  $\sigma$ -donor capabilities on the metal increase the electron density on the phosphorus atom, raise the  $\pi^*$ -orbital energy, and enhance its nucleophilicity. Spectator ligands with strong  $\pi$ -acceptor capabilities lower the charge concentration on P and stabilize the  $\pi^*$ -orbital, which results in a higher affinity for electron-rich species. The  $ML_n=PH$  bond is investigated using a bond energy analysis in terms of electrostatic interaction, Pauli repulsion, and orbital interaction. A symmetry decomposition scheme affords a quantitative estimate of the  $\sigma$ - and  $\pi$ -bond strengths. It is shown that the investigated phosphinidenes are strong  $\pi$ -acceptors and even stronger  $\sigma$ -donors. The metal-phosphinidene interaction increases on going from the first to the second- and third-row transition metals.

Phosphinidenes, stabilized by transition metal complexes ( $L_n$ -MPR), are a rapidly growing class of viable reagents in phosphoorganic chemistry. Their properties and behavior relate to those of carbenes and support the notion that low-coordinate phosphorus compounds mimic the chemistry of their related hydrocarbons remarkably well.<sup>1</sup> In analogy with the transition metal-complexed carbenes, it is attractive to classify the phosphinidene complexes as electrophilic and nucleophilic. Such a generalized distinction for the carbene complexes  $L_nMCR_2$  is made in terms of Fischer- and Schrock-type complexes and depends on the carbene substituent R, the choice of the transition metal M, its oxidation state, and the nature of its ligands L.<sup>2</sup> Is a similar distinction also appropriate for the complexed phosphinidenes? The literature of the past two decades does suggest the existence of phosphinidenes with rather different properties.

In the early 1980s, Mathey and co-workers developed a convenient chelotropic route for the in situ generation of phosphinidenes stabilized by a terminal  $M(CO)_5$  ( $M = Cr, Mo, W$ ) group.<sup>3</sup> The latest representative in this group is  $(OC)_4Fe=PNR_2$ , which is formed in situ by a condensation reaction.<sup>4,5</sup>

Complexes of the general type  $(OC)_nM=PR$  are characterized by their high reactivity and short lifetime. So far, these reactive intermediates have eluded direct observation. However, their chemical reactivity toward, for example, alkenes and alkynes, is indicative of electrophilic behavior of singlet-state species. The analogy of the  $M(CO)_n$ -complexed phosphinidenes with Fischer carbenes is appealing despite their difference in stability.<sup>6</sup> The stability increases with a  $Cp^*$  ligand. This is illustrated by the recently reported crystal structures of the cationic complexes  $[Cp^*(OC)_nM=PNR_2][AlCl_4]$  ( $M = W, Ru; n = 3, 2$ ), which display electrophilic behavior.<sup>7</sup>

Remarkably stable neutral transition metal-complexed phosphinidenes are also known. For example, crystal structures were reported for the bis(cyclopentadienyl)molybdenum,<sup>8</sup>-tungsten,<sup>9</sup> and -zirconium<sup>10</sup> complexes  $(Cp_2M)=PR$  as well as for the polydentate-tantalum complex  $(N_3N)Ta=PR$  [ $N_3N = (Me_3SiNCH_2CH_2)_3N, R = Ph, Cy, t-Bu$ ].<sup>11</sup> The reactivity of these phosphinidenes differs substantially from those that are complexed by the  $M(CO)_n$  group. Illustrative is the reaction with aldehydes, which results in phosphoalkenes, while no addition

- (1) (a) Regitz, M.; Scherer, O. J., Eds. *Multiple Bonds and Low Coordination in Phosphorus Chemistry*; Georg Thieme Verlag: Stuttgart, 1991. (b) Dillon, K. D.; Mathey, F.; Nixon, J. F. *Phosphorus: The Carbon Copy*; Wiley: Chichester, U.K., 1998.
- (2) (a) Vyboishchikov, S.; Frenking, G. *Chem. Eur. J.* **1998**, *4*, 1428. (b) Nugent, W. A.; Mayer, J. M. *Metal-Ligand Multiple Bonds*; Wiley: New York, 1988. (c) Dötz, K. H.; Fischer, H.; Hofmann, P.; Kreissl, F. R.; Schubert, U.; Weiss, K. *Transition Metal Carbene Complexes*; VCH: Weinheim, 1983. (d) Hill, A. F.; Roper, W. R.; Waters, J. M.; Wright, A. H. *J. Am. Chem. Soc.* **1983**, *105*, 5939. (e) Schrock, R. R. *Acc. Chem. Res.* **1979**, *12*, 98.
- (3) (a) Marinetti, A.; Mathey, F.; Fischer, J.; Mitschler, J. *J. Chem. Soc., Chem. Commun.* **1982**, 667. (b) Marinetti, A.; Mathey, F. *Organometallics* **1982**, *1*, 1488. (c) Marinetti, A.; Mathey, F. *Organometallics* **1984**, *3*, 456.
- (4) King, R. B.; Wu, F. J.; Holt, E. M. *J. Am. Chem. Soc.* **1993**, *109*, 7764.

- (5) (a) Wit, J. B. M.; van Eijkel, G. T.; Schakel, M.; Lammertsma, K. *Tetrahedron* **2000**, *56*, 137. (b) Wit, J. B. M.; van Eijkel, G. T.; de Kanter, F. J. J.; Schakel, M.; Ehlers, A. W.; Lutz, M.; Spek, A. L.; Lammertsma, K. *Angew. Chem., Int. Ed.* **1999**, *38*, 2596.
- (6) Frison, G.; Mathey, F.; Sevin, A. *J. Organomet. Chem.* **1998**, *570*, 225.
- (7) (a) Sterenberg, B. T.; Udachin, K. A.; Carty, A. J. *Organometallics* **2001**, *20*, 2657. (b) Sterenberg, B. T.; Udachin, K. A.; Carty, A. J. *Organometallics* **2001**, *20*, 4463.
- (8) Hitchcock, P. B.; Lappert, M. F.; Leung, W.-P. *J. Chem. Soc., Chem. Commun.* **1987**, 1282.
- (9) Bohra, R.; Hitchcock, P. B.; Lappert, M. F.; Leung, W.-L. *Polyhedron* **1989**, *8*, 1884.
- (10) Hou, Z.; Breen, T. L.; Stephan, D. W. *Organometallics* **1993**, *12*, 3158.
- (11) Cummins, C. C.; Schrock, R. R.; Davis, W. M. *Angew. Chem.* **1993**, *105*, 758.

to olefins has been observed. This nucleophilic behavior suggests a similarity with the Schrock carbenes.<sup>12</sup>

What drives this distinction in properties of the phosphinidenes? Can a classification be applied analogous to the Fischer- and Schrock-type carbene complexes? For example, the transition metal of the electrophilic (OC)<sub>5</sub>W=PR is in a low oxidation state, while the nucleophilic (N<sub>3</sub>N)Ta=PR contains an early transition metal in a high oxidation state. However, the spectator ligand can be of equal or of even more importance. For example, replacing the CO ligands in (OC)<sub>5</sub>Mo=PR for cyclopentadienyl groups while maintaining the same transition metal, as in Cp<sub>2</sub>-Mo=PR, changes the behavior from electrophilic to nucleophilic.

The pivotal issue we address in this investigation is how the chemical behavior of phosphinidene complexes may be tuned by modifying the transition metal and its ligands. Our primary aim is to determine what distinguishes electrophilic from nucleophilic phosphinidene complexes. Answering this question requires insight into the influence of the transition metal group on the phosphorus atom, which can be obtained with density functional theoretical (DFT) methods. DFT studies have been applied successfully to highlight the influence of both the M(CO)<sub>5</sub> (M = Cr, Mo, W) group and the  $\pi$ -donating P-R substituent on the singlet-triplet splitting of phosphinidenes.<sup>13</sup> The applicability of the DFT method for these systems has been supported by an ab initio study using high-level correlation schemes.<sup>14</sup> In the present study, we will use the DFT method first to rationalize the electrophilic versus nucleophilic behavior using the electronic structures of the (OC)<sub>4</sub>Fe=PR and (Cp<sub>2</sub>-Cr)=PR complexes, respectively. Next we will investigate a broad spectrum of phosphinidene complexes containing the CO, phosphine (PH<sub>3</sub>), and cyclopentadienyl (Cp) ligands to establish whether they fall into one of the extreme categories or exhibit a gradual transition from nucleophilicity to electrophilicity. Finally, we will examine the changes on going from the first- to the second- to the third-row transition metals.

## Method

**General Procedure.** The calculations were carried out using the parallelized Amsterdam density functional (ADF) program.<sup>15</sup> The MOs were expanded in a large, uncontracted set of Slater-type orbitals (STOs) containing polarization functions. The used TZP basis set is of triple- $\zeta$  quality for all atoms and has been augmented with one set of 4p functions for each transition metal atom and one set of d-polarization functions for each main group atom.<sup>16</sup> The 1s core shell of carbon and oxygen and the 1s2s2p core shells of phosphorus were treated by the frozen-core (FC) approximation. The metal centers were described by an uncontracted triple- $\zeta$  STO basis set for the outer *ns*, *np*, *nd*, (*n* + 1)*s*, (*n* + 1)*p* orbitals and in the case of the third-row transition metals also for the 4*f* orbitals, whereas the shells of lower energy were treated by the frozen core approximation. An auxiliary set of *s*, *p*, *d*, *f*, and *g* STOs, centered on all nuclei, was used to fit the molecular density and to represent the Coulomb and exchange potentials accurately in each

self-consistent field (SCF) cycle.<sup>17</sup> The numerical integration and the calculation of the VDD charges was done with the scheme developed by te Velde and Baerends.<sup>18</sup>

All calculations were performed at the nonlocal exchange self-consistently (NL-SCF) level, using the local density approximation (LDA) in the Vosko-Wilk-Nusair parametrization<sup>19</sup> with nonlocal corrections for exchange<sup>20</sup> and correlation (BP).<sup>21</sup> All geometries were optimized using the analytical gradient method implemented by Versluis and Ziegler<sup>22</sup> including relativistic effects by the ZORA approximation.<sup>23</sup>

**Bonding Energy Analysis.** The transition metal-phosphorus bond is analyzed by decomposing the interaction energy in an exchange (or Pauli) repulsion plus electrostatic interaction energy part ( $\Delta E^{\text{elst}}$ ) and an orbital interaction energy (charge transfer, polarization).<sup>24</sup> Usually fragments need to be prepared for interaction, either by deforming them from their equilibrium structure to the geometry they acquire in the overall molecule or by electronic excitation to a "valence state" electronic configuration. The overall bond energy  $\Delta E$  is thus made up of three major components:

$$\Delta E = \Delta E^{\text{prep}} + \Delta E^{\circ} + \Delta E^{\text{oi}} \quad (1)$$

where

$$\Delta E^{\circ} = \Delta E^{\text{elst}} + \Delta E^{\text{Pauli}}$$

Note that  $\Delta E$  is defined as the negative of the bond dissociation energy (BDE), i.e.,  $\Delta E = E(\text{molecule}) - E(\text{fragments})$ , thereby giving negative values for stable bonds.  $\Delta E^{\text{elst}}$  represents the usually attractive electrostatic interaction between the prepared fragments when they are put (with unchanged electron densities) at the positions they occupy in the complex. The Pauli repulsion term  $\Delta E^{\text{Pauli}}$  consists of the four-electron destabilizing interactions between occupied orbitals and is responsible for the steric repulsion. For neutral fragments,  $\Delta E^{\text{elst}}$  and  $\Delta E^{\text{Pauli}}$  are usually combined in the term  $\Delta E^{\circ}$  (eq 1). The orbital interaction  $\Delta E^{\text{oi}}$  accounts for charge transfer (interaction between occupied and unoccupied orbitals on the two fragments) and polarization (empty/occupied orbital mixing on one fragment). We will not try to separate charge-transfer and polarization components, but will use the extended transition state (ETS) method developed by Ziegler and Rauk to decompose the  $\Delta E^{\text{oi}}$  term into contributions from each irreducible representation of the interacting system. In systems with a clear  $\sigma$ ,  $\pi$ -separation, this symmetry partitioning proves to be most informative.

## Results and Discussion

The presentation of the data is as follows. First we discuss two typical cases, an electrophilic phosphinidene complex, (OC)<sub>4</sub>Fe=PH, and a nucleophilic one, Cp<sub>2</sub>Cr=PH. Next we compare the computed structures and reactivities for a selected group of phosphinidene complexes including a comparison with reported X-ray crystal structures and observed reaction behavior. Finally, we evaluate the ligand (CO, PH<sub>3</sub>, Cp) substitution for all the first-, second-, and third-row transition metal complexes.

- (12) Cowley, A. H. *Acc. Chem. Res.* **1997**, *30*, 445.  
 (13) Ehlers, A. W.; Lammertsma, K.; Baerends, E. J. *Organometallics* **1998**, *17*, 2738.  
 (14) (a) Creve, S.; Pierloot, K.; Nguyen, M. T.; Vanquickenborne, L. G. *Eur. J. Inorg. Chem.* **1999**, 107. (b) Creve, S.; Pierloot, K.; Nguyen, M. T. *Chem. Phys. Lett.* **1998**, *185*, 429.  
 (15) (a) Fonseca-Guerra, C.; Visser, O.; Snijders, J. G.; te Velde, G.; Baerends, E. J. In METECC-95, Clementi, E., Corongiu, C. Eds.; Cagliari, 1995; p 307. (b) Baerends, E. J.; Ellis, D. E.; Ros, P. *Chem. Phys.* **1973**, *2*, 41.  
 (16) (a) Snijders, J. G.; Baerends, E. J.; Vernooijs, P. *At. Nucl. Data Tables* **1982**, *99*, 84. (b) Snijders, J. G.; Vernooijs, P.; Baerends, E. J. Internal report, Free University of Amsterdam, The Netherlands, 1981.

- (17) Krijn, K.; Baerends, E. J. Internal report, Free University of Amsterdam, The Netherlands, 1984.  
 (18) (a) te Velde, G.; Baerends, E. J. *J. Comput. Phys.* **1992**, *99*, 84. (b) Bickelhaupt, F. M.; van Eikema Hommes, N. J. R.; Fonseca Guerra, C.; Baerends, E. J. *Organometallics* **1996**, *15*, 2923.  
 (19) Vosko, S. H.; Wilk, L.; Nusair, M. *Can. J. Phys.* **1980**, *58*, 1200.  
 (20) Becke, A. D. *Phys. Rev. A* **1988**, *38*, 3098.  
 (21) Perdew, J. P. *Phys. Rev. B* **1986**, *33*, 8822.  
 (22) (a) Fan, L.; Versluis, L.; Ziegler, T.; Baerends, E. J.; Raveneck, W. *Int. J. Quantum. Chem.; Quantum. Chem. Symp.* **1988**, *S22*, 173. (b) Versluis, L.; Ziegler, T. *Chem. Phys.* **1988**, *322*, 88.  
 (23) van Lenthe, E.; Ehlers, A. W.; Baerends, E. J. *J. Chem. Phys.* **1999**, *110*, 8943.  
 (24) (a) Morokuma, K. *Acc. Chem. Res.* **1977**, *10*, 244. (b) Ziegler, T.; Rauk, A. *Inorg. Chem.* **1979**, *18*, 1755. (c) Ziegler, T.; Rauk, A. *Theor. Chim. Acta* **1977**, *46*, 1.

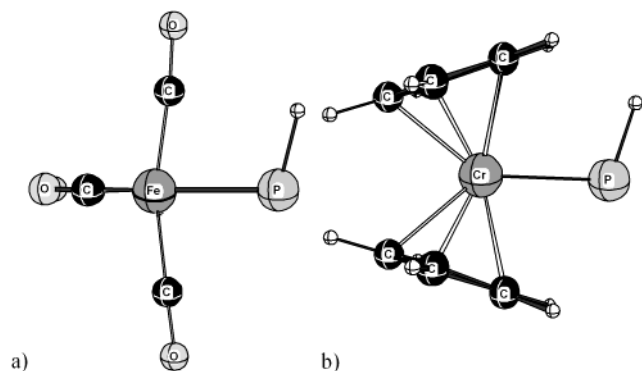


**Figure 1.** Optimized structures of (a)  $Fe(CO)_4=PH$  and (b)  $CrCp_2=PH$ .

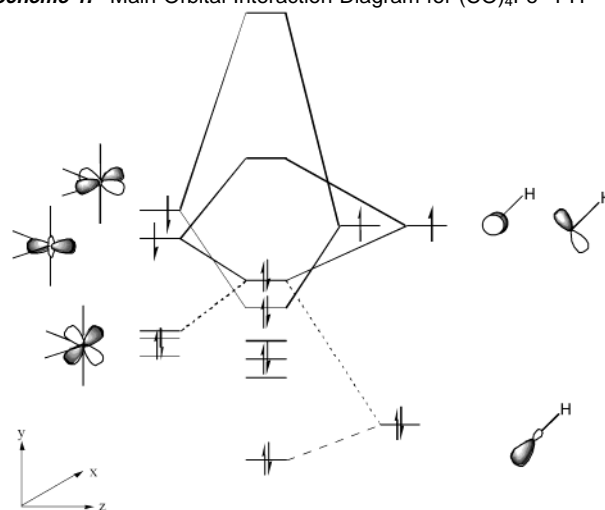
**I. Electrophilic versus Nucleophilic Reactivity. (A) Electrophilic Phosphinidene Complex  $(OC)_4Fe=PH$ .** The transient  $P-NiPr_2$  derivative of this complex, which is synthesized in situ from  $^iPr_2NPCl_2$  and Collman's reagent ( $Na_2Fe(CO)_4$ ), adds to alkynes and olefins below  $0\text{ }^\circ C$ . Evidently, it possesses electrophilic character despite its electron-donating amine substituent. So far, it is the only reported derivative with a complexing  $Fe(CO)_4$  group. A broader spectrum of derivatives is known for the electrophilic  $(OC)_5MPR$  ( $M = W, Mo, Cr$ ) phosphinidenes. These reagents typically require higher temperatures for their generation (about  $100^\circ$  without and  $60\text{ }^\circ C$  with  $CuCl$  as catalyst). Theoretical studies showed a stabilizing influence of the  $NH_2$  group versus the  $H, CH_3,$  and  $Ph$  groups, for both  $M(CO)_5$  complexed and "free" phosphinidenes. We focus on the parent iron complex because of its simpler orbital analysis as will become evident.

**Geometry.** The optimized geometry of  $(OC)_4Fe=PH$ , shown in Figure 1a, has a distorted trigonal bipyramidal form with the phosphinidene group in the equatorial plane of the transition metal. The  $P-H$  bond is in an eclipsed conformation with one of the axial COs. The two axial CO ligands are slightly bent ( $\angle C-Fe-C = 164.1^\circ$ ) toward the phosphorus. Rather small values are calculated for the  $Fe-P-H$  angle of  $104.9^\circ$  and the  $Fe=P$  bond distance of  $2.192\text{ \AA}$ . This distance is even shorter than the earlier reported calculated  $Cr=P$  distance of  $2.271\text{ \AA}$  for  $(OC)_5Cr=PH$ , which was interpreted to possess significant double bond character.<sup>13</sup> Unfortunately, there are no experimental data available for comparison.

**MO Interaction Diagram.** To establish the orbital interactions for the iron complex, we construct a qualitative MO diagram from the  $Fe(CO)_4$  and  $PH$  fragments, both of which have triplet ground states.<sup>13,25</sup> The diagram is given in Scheme 1. It shows the preformed  $Fe(CO)_4$  fragment ( $C_{2v}$  symmetry) in its typical  $d^8$  configuration with two unpaired electrons in the  $d_{z^2}$  and  $d_{xy}$  hybrid orbitals of iron. The  $^3Fe(CO)_4$  is calculated to be  $17.9\text{ kcal/mol}$  more stable than the corresponding closed-shell singlet state.

The  $^3PH$  fragment is depicted with one electron in each of the degenerate  $p_x$  and  $p_z$  orbitals; the  $^1PH - ^3PH$  energy difference amounts to  $34.8\text{ kcal/mol}$  in favor of the triplet state. The main feature of the orbital interaction diagram is that the singly occupied orbitals of both the fragments are of similar energy. One-electron energies of  $5.47\text{ eV}$  are calculated for those of  $PH$  and  $5.20$  ( $d_{z^2}$ ) and  $5.60$  ( $d_{xy}$ )  $eV$  for those of  $Fe(CO)_4$ . This similarity in fragment orbital energies suggests that little,

**Scheme 1.** Main Orbital Interaction Diagram for  $(CO)_4Fe=PH$



if any, net charge transfer takes place between the  $P$  and  $Fe$  atoms in the phosphinidene complex.

**Atomic Charges.** Indeed, the calculated VDD charge<sup>18</sup> of only  $-0.060e$  on the phosphorus atom supports the depicted view; all atomic charges are given in Table 1. Whereas the magnitude and mathematical sign of calculated partial charges are not directly related to observable quantities, a comparison within a series of similar structures, however, shows trends that can be related to physical and chemical properties. We shall pursue this comparative analysis in the following sections.

**(B) Nucleophilic Phosphinidene Complex  $Cp_2Cr=PH$ .** The  $P$ -supermesityl ( $2,4,6\text{-}tBu_3-C_6H_2$ )-substituted derivatives of the heavier  $Mo$  and  $W$  congeners of this complex are both reported to be stable compounds, much in contrast to the transient electrophilic metal-carbonyl complexes. The crystallographically determined short  $Mo=P$  bond distance of  $2.370(2)\text{ \AA}$  with a rather bent phosphorus ( $\angle MoPC = 115.8(2)^\circ$ ) suggests double bond character despite the bulkiness of the supermesityl group. The  $^{31}P$  NMR resonance of the  $WCp_2$  complex at  $661.1\text{ ppm}$  has a surprisingly small  $^1J(P,W)$  coupling constant of  $153\text{ Hz}$ ,<sup>8</sup> suggesting a rather negatively charged phosphorus. We chose the parent nucleophilic system of the lighter, "first-row"  $Cp_2Cr$  complex for our analysis.

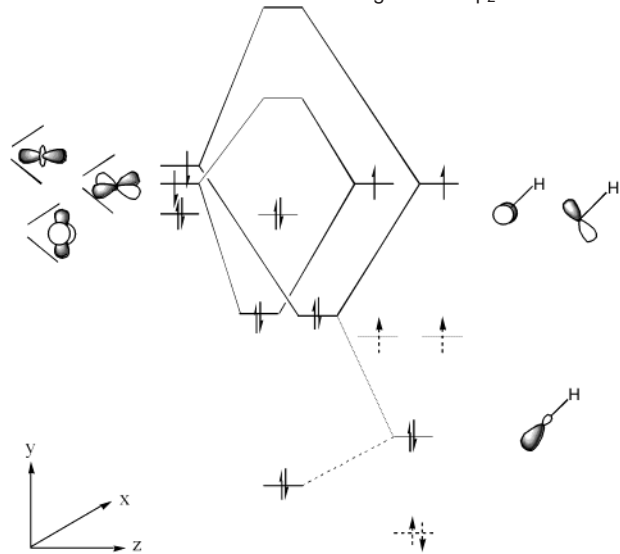
**Geometry.** The optimized typical sandwich-like geometry of  $Cp_2Cr=PH$  ( $C_s$  symmetry), shown in Figure 1b, has a rather short  $Cr=P$  bond length of  $2.289\text{ \AA}$  with a  $Cr-P-H$  angle of  $106.8^\circ$ , both of which are indicative of double bond behavior. The  $CrP$  bond length is only modestly longer than the  $2.271\text{ \AA}$  for the electrophilic  $(OC)_5Cr=PH$ .<sup>13</sup> Analogous to the crystallographic structure of  $Cp_2Mo=PMes^*$ , the  $PH$  bond in the parent  $CrCp_2$  structure is in an eclipsed conformation with one of the  $Cp$  ligands. The  $Cp-Cr-Cp$  angle of  $147.4^\circ$  is also similar to the experimental value of  $144.6^\circ$  for the  $Mo$  structure.<sup>8</sup>

**MO Interaction Diagram.** Again we construct a molecular interaction diagram from the  $Cp_2Cr$  and  $PH$  fragments to inspect the electronic properties of the complex (Scheme 2). Like  $Fe(CO)_4$ , the  $Cp_2Cr$  fragment also has a preferred triplet ground state as well, making a comparison straightforward. Since the chromium atom in  $Cp_2Cr$  is formally doubly charged ( $+2$ ), a typical  $d^4$  configuration results. Two electrons are in the doubly occupied  $d_{x^2-y^2}$  orbital, which lies in the plane separating the two cyclopentadienyl rings. The other two  $d$  electrons are



**Table 1.** Calculated VDD Charges on the Phosphorus Atom of Phosphinidene Complexes  $ML_r=PH$ 

$Cp_2Ti=PH$ −0.270	$Cp_2Cr=PH$ −0.220	$Cp(PH_3)_3V=PH$ −0.210	$Cp(PH_3)Co=PH$ −0.170	$Cp(CO)Co=PH$ −0.118	$Cp(CO)_3V=PH$ −0.081	$(CO)_4Fe=PH$ −0.060
$Cp_2Zr=PH$ −0.295	$Cp_2Mo=PH$ −0.239	$Cp(PH_3)_3Nb=PH$ −0.243	$Cp(PH_3)Rh=PH$ −0.153	$Cp(CO)Rh=PH$ −0.145	$Cp(CO)_3Nb=PH$ −0.137	$(CO)_4Ru=PH$ −0.109
$Cp_2Hf=PH$ −0.323	$Cp_2W=PH$ −0.236	$Cp(PH_3)_3Ta=PH$ −0.234	$Cp(PH_3)Ir=PH$ −0.151	$Cp(CO)Ir=PH$ −0.146	$Cp(CO)_3Ta=PH$ −0.144	$(CO)_4Os=PH$ −0.124

**Scheme 2.** Main Orbital Interaction Diagram for  $Cp_2Cr=PH^a$ 

<sup>a</sup> The dashed lines for PH indicate its orbital energies at infinite separation from  $Cp_2Cr$ .

divided over the  $d_{z^2}$  and  $d_{xz}$  orbitals, which are in the direction of the triplet PH fragment.  $Cr=P$  double bond character results from the combined  $\sigma$  ( $P(p_z)-Cr(d_{z^2})$ ) and  $\pi$  ( $P(p_x)-Cr(d_{xz})$ ) interactions. The  $\pi$ -interaction forces the P-substituent into the sterically most hindered position, i.e., pointing toward one of the cyclopentadienyl rings.

The important feature distinguishing the interaction diagram of  $Cp_2Cr=PH$  from that of  $(OC)_4Fe=PH$  is the much larger difference in energies between the singly occupied orbitals of the fragments. For the equilibrium geometries of the two fragments (at infinite distance), these energies are  $-3.10$  eV for  $Cp_2Cr$  and  $-5.47$  eV for PH; the energy diagram is depicted in Scheme 2. It is then not surprising that upon bond formation the PH fragment acts as an electron acceptor, causing significant charge to transfer from the metal to the phosphorus atom. Consequently, the PH fragment orbitals increase in energy and this is illustrated in Scheme 2. The transfer of charge seems to have less influence on the Cr orbitals, since the energy of the  $d_{x^2-y^2}$  orbital, which shows no mixing with other orbitals, remains almost unchanged.

**Atomic Charges.** That indeed significant transfer of charge takes place is evident from the calculated charge of  $-0.220e$  on the phosphorus atom. This charge is substantially more than the  $-0.060e$  calculated for the  $Fe(CO)_4$  complex. Hence, the relatively negatively charged phosphorus of  $Cp_2Cr=PH$  agrees with its nucleophilic character.

**(C) M=P Bond Strengths.** In preparation of an evaluation of the bond strength between phosphorus and all of the first-, second-, and third-row transition metals of the phosphinidene complexes, we determine in this section first those for the discussed  $(OC)_4Fe=PH$  and  $Cp_2Cr=PH$ . Computation of their

BDEs is readily performed as the fragments are already available from the MO interaction analysis. The choice of the electronic ground state of all species involved is crucial. We emphasize again that the BDE analysis of the two (singlet) phosphinidene complexes is straightforward because their fragments have strongly favored triplet ground states. In this context, it is worth noting that an analysis of the BDE of  $(OC)_5Cr=PH$  is less straightforward as the  $Cr(CO)_5$  fragment has a preferred singlet ground state. Consequently, dissociating such a complex in either singlets (S) or triplets (T) would require incorporating T→S or S→T relaxation energies for  $Cr(CO)_5$  or PH, respectively. As noted, this S→T relaxation energy is a significant  $34.8$  kcal/mol for the free phosphinidene.

**$(OC)_4Fe=PH$ .** The singly occupied PH orbitals contribute equally,  $\sim 45\%$  each, to the  $\sigma$ - and  $\pi$ -bonding orbitals of the complex, which are its highest occupied orbitals and separated by only  $0.42$  eV (Scheme 1). A reasonable participation of  $\pi$ -character to the  $Fe=P$  bonding seems plausible. Indeed, the orbital interaction energy  $\Delta E^{oi}$  has a significant  $\Delta E_{\pi}$  component of  $-32.2$  kcal/mol besides a strong  $\Delta E_{\sigma}$  contribution of  $-90.7$  kcal/mol. Together with the interaction energy  $\Delta E^{\circ}$  of  $+55.3$  kcal/mol and the small preparation energy  $\Delta E^{prep}$  of  $+6.0$  kcal/mol for the fragments, this results in a final BDE of  $-61.6$  kcal/mol.

**$Cp_2Cr=PH$ .** This complex has a slightly different bonding arrangement (Scheme 2). The PH fragment's contribution of  $\sim 60\%$  to the highest occupied MO with  $\sigma$ -bond character, the HOMO-1 ( $A'$  symmetry), comes largely from its singly occupied  $p_z$  orbital with some participation of the phosphorus lone pair orbital. This mixing-in of the lone pair represents a slight shift from  $sp$  toward  $sp^2$  hybridization on complexation of the phosphinidene. The  $\pi$ -bonding orbital ( $A''$  symmetry) is more balanced as the singly occupied  $p_x$  (P) and  $d_{xz}$  (Cr) orbitals contribute equally. Compared to the  $(OC)_4Fe=PH$  complex, this bonding arrangement translates into a smaller  $\Delta E_{\sigma}$  component ( $-79.5$  kcal/mol), but with nearly equal contributions from  $\Delta E_{\pi}$  ( $-30.0$  kcal/mol),  $\Delta E^{\circ}$  ( $+53.3$  kcal/mol), and  $\Delta E^{prep}$  ( $+17.1$  kcal/mol). Consequently, a smaller BDE of  $-39.1$  kcal/mol results. However, it is evident that both the electrophilic  $(OC)_4Fe=PH$  and the nucleophilic  $Cp_2Cr=PH$  have double bonds between the transition metal and the phosphorus.

**(D) Charge Control and Orbital Control.** We showed that the charges on the phosphorus atoms of  $(OC)_4Fe=PH$  and  $Cp_2Cr=PH$  are rather different from each other due to the different frontier orbital energies of their transition metal fragments. This transfer of charge (*charge control*) is significant for the nucleophilic  $Cp_2Cr=PH$ . However, the reactivity of a phosphinidene complex also depends on its orbital energies (*orbital control*). Nucleophilic phosphinidenes are expected to have a filled donor orbital of high energy (HOMO) and electrophilic ones a low-lying empty acceptor orbital (LUMO). This is indeed the case.

Thus, the theoretically predicted energy of  $-4.4$  eV for the LUMO of  $(OC)_4Fe=PH$ , which is the  $\pi^*$ -orbital formed from an antibonding combination of the phosphorus  $p_x$  orbital and the metal  $d_{xz}$  orbital, is much lower in energy than that for  $Cp_2Cr=PH$  ( $-2.2$  eV). Likewise, the orbital energy of  $-4.4$  eV for the phosphorus lone pair in  $Cp_2Cr=PH$  is much higher in energy than that for the corresponding orbital in  $(OC)_4Fe=PH$  ( $-6.4$  eV). How can this harmony between charge control and orbital control be rationalized?

On  $P=M$  bond formation,  $PH$  acts as an electron acceptor when the metal moiety has high-lying frontier orbitals (i.e.,  $Cp_2Cr$ ); charge will transfer from the metal to phosphorus. As a result, the orbitals of the phosphinidene fragment rise in energy, which explains the relatively high energy of the phosphorus lone pair and hence its enhanced nucleophilicity. Simultaneously, the singly occupied orbitals of  $PH$  destabilize in the effective field of its enhanced negative charge, thereby reducing the energy gap with the  $d$  orbitals of the metal fragment, which consequently increases the interaction with these orbitals. In fact, the interaction between the phosphorus  $p_x$  orbital and the  $d_{xz}$  orbital of the metal fragment is of comparable strength for the two metal fragments  $Fe(CO)_4$  and  $CrCp_2$ . The interaction destabilizes the high-lying  $d_{xz}$  orbital of  $Cp_2Cr$ , which is  $\sim 2.5$  eV higher in energy than that of  $Fe(CO)_4$ , resulting in an antibonding  $\pi^*$  ( $p_x-d_{xz}$ ) LUMO of  $Cp_2Cr=PH$  that is 2.2 eV higher in energy than the  $\pi^*$  LUMO of  $(OC)_4Fe=PH$ . Evidently, also orbital control suggests  $Cp_2Cr=PH$  to have nucleophilic character and identifies  $(OC)_4Fe=PH$  as electrophilic.

**II. Ligand Variation for the First-Row Transition Metal Groups.** So far, we have seen that electrophilic and nucleophilic phosphinidene complexes can be distinguished from each other by the relative energies of the highest (singly) occupied orbitals of the transition metal fragment. We have also seen that as a result the charge on the phosphorus atom differs for these complexes. What influences the orbital energies most? Is it the choice of the transition metal, its ligands, or both? And how adequate does the calculated charge on phosphorus reflect this influence?

To answer these questions, we apply Hoffmann's isolobal approach<sup>26</sup> to the transition metals of the first row. We consider three ligands with different properties, namely, the  $6e$   $\eta^5$ -donor  $Cp^-$ , the  $2e$   $\sigma$ -donor/ $2e$   $\pi$ -acceptor  $CO$ , and  $PH_3$ , which is a moderate  $\sigma$ -donor and weak  $\pi$ -acceptor  $2e$  ligand.<sup>27</sup> Moreover, we will consider only neutral systems. Consequently, replacing the negatively ( $-1$ ) charged  $Cp$  ring for three  $CO$  ligands requires also a change of transition metal, to a column to the left in the periodic table.

Thus,  $Cp(OC)Co=PH$  and  $(OC)_4Fe=PH$  are isolobal as are  $Cp_2Cr=PH$  and  $Cp(OC)_3V=PH$ . Furthermore, this row of investigated transition metal phosphinidene complexes has been extended with the group IV bis(cyclopentadienyl) complexes. These compounds are  $16e^-$  complexes and differ from the group VI analogues by their unoccupied  $d_{x^2-y^2}$  orbital. However, the Zr congener is known for its nucleophilic reactivity and the  $16e^-$  complex  $Cp_2Zr=PR$  can be isolated if it is stabilized by an extra trimethylphosphine ligand.<sup>10</sup> The X-ray structure shows a rather

**Table 2.** Selected Bond Lengths ( $\text{\AA}$ ) and Angles (deg) of Phosphinidene Complexes  $ML_n=PH$

	$Cp_2Ti=PH$	$Cp_2Zr=PH$	$Cp_2Hf=PH$
M–P	2.352	2.473	2.456
P–H	1.448	1.444	1.445
M–Cp <sub>anti</sub>	2.055	2.229	2.188
M–Cp(2)	2.042	2.230	2.192
H–P–M	104.2	100.4	100.2
P–M–Cp(1)	104.9	103.8	104.6
P–M–Cp(2)	111.3	111.9	113.1
	$Cp_2Cr=PH$	$Cp_2Mo=PH$	$Cp_2W=PH$
M–P	2.286	2.377	2.379
P–H	1.453	1.447	1.446
M–Cp <sub>anti</sub>	1.845	1.998	1.981
M–Cp(2)	1.834	1.992	1.980
H–P–M	106.8	103.6	103.1
P–M–Cp(1)	103.6	102.7	103.1
P–M–Cp(2)	108.9	110.0	110.7
	$Cp(CO)Co=PH$	$Cp(CO)Rh=PH$	$Cp(CO)Ir=PH$
M–P	2.090	2.203	2.216
P–H	1.451	1.450	1.451
M–Cp(1)	1.728	1.961	1.973
M–L	1.725	1.862	1.850
M–P–H	106.6	105.9	105.1
P–M–Cp(1)	133.5	133.6	132.5
P–M–L	90.1	88.9	90.8
	$Cp(PH_3)Co=PH$	$Cp(PH_3)Rh=PH$	$Cp(PH_3)Ir=PH$
M–P	2.085	2.195	2.210
P–H	1.463	1.462	1.465
M–Cp(1)	1.705	1.949	1.950
M–L	2.113	2.234	2.226
M–P–H	107.1	106.7	105.9
P–M–Cp(1)	133.9	4.7	135.1
P–M–L	91.4	88.8	90.0
	$Cp(CO)_3V=PH$	$Cp(CO)_3Nb=PH$	$Cp(CO)_3Ta=PH$
M–P	2.307	2.440	2.436
P–H	1.446	1.441	1.441
M–Cp(1)	1.980	2.172	2.150
M–L	1.938	2.114	2.091
M–L'	1.933	2.093	2.073
M–P–H	106.5	106.2	105.6
P–M–Cp(1)	114.4	112.0	111.9
P–M–L	126.6	126.7	127.3
Cp(1)–M–L'	127.2	129.4	128.9
	$Cp(PH_3)_3V=PH$	$Cp(PH_3)_3Nb=PH$	$Cp(PH_3)_3Ta=PH$
M–P	2.326	2.441	2.434
P–H	1.451	1.449	1.447
M–Cp(1)	1.993	2.165	2.140
M–L	2.414	2.563	2.538
M–L'	2.362	2.506	2.486
M–P–H	105.9	105.0	104.2
P–Mn–Cp(1)	108.9	106.9	107.5
P–M–L	139.8	140.2	140.4
Cp(1)–M–L'	126.2	129.6	129.4
	$(CO)_4Fe=PH$	$(CO)_4Ru=PH$	$(CO)_4Os=PH$
M–P	2.192	2.317	2.337
P–H	1.447	1.445	1.445
M–CO <sub>ax</sub> (1)	1.817	1.973	1.972
M–CO <sub>ax</sub> (2)	1.797	1.953	1.960
M–CO <sub>eq</sub>	1.793	1.944	1.940
M–P–H	104.9	102.6	101.9
P–Mn–CO <sub>eq</sub>	130.2	131.3	131.4

long distance of  $2.74$   $\text{\AA}$  for this additional ligand. We did not include the apparent weak interaction with additional ligands in our survey.

(25) Poliakoff, M.; Turner, J. J. *J. Chem. Soc., Dalton Trans.* **1974**, 2276.

(26) Hoffmann, R. *Angew. Chem.* **1982**, *94*, 725.

(27) Gonzales-Blanco, O.; Branchadell, V. *Organometallics* **1997**, *16*, 5556.

**Table 3.** Calculated Energy Levels (in eV) for the Singly Occupied Orbitals of the Transition Metal Fragments  $ML_n$ 

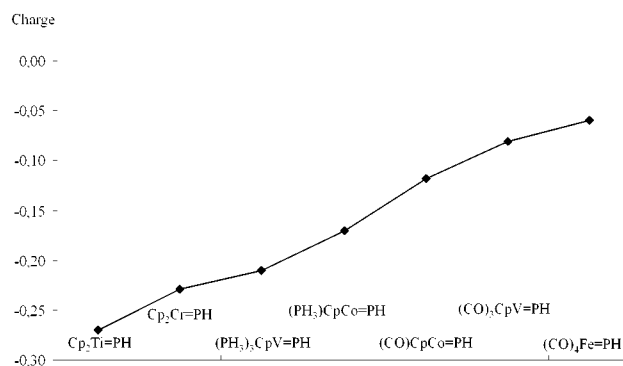
	Cp <sub>2</sub> Ti	Cp <sub>2</sub> Cr	Cp(PH <sub>3</sub> ) <sub>3</sub> V	Cp(PH <sub>3</sub> )Co	Cp(CO)Co	Cp(CO) <sub>3</sub> V	(CO) <sub>4</sub> Fe
a'	-2.95	-3.10	-2.86	-3.27	-4.01	-4.36	-5.20
a''	-3.21	-3.10	-3.47	-3.47	-4.39	-5.34	-5.60
	Cp <sub>2</sub> Zr	Cp <sub>2</sub> Mo	Cp(PH <sub>3</sub> ) <sub>3</sub> Nb	Cp(PH <sub>3</sub> )Rh	Cp(CO)Rh	Cp(CO) <sub>3</sub> Nb	(CO) <sub>4</sub> Ru
a'	-2.88	-2.96	-2.81	-3.31	-3.90	-4.26	-4.93
a''	-2.63	-3.28	-3.48	-3.57	-4.45	-5.24	-5.23
	Cp <sub>2</sub> Hf	Cp <sub>2</sub> W	Cp(PH <sub>3</sub> ) <sub>3</sub> Ta	Cp(PH <sub>3</sub> )Ir	Cp(CO)Ir	Cp(CO) <sub>3</sub> Ta	(CO) <sub>4</sub> Os
a'	-2.84	-2.95	-2.78	-3.39	-4.11	-4.22	-4.93
a''	-2.40	-3.19	-3.47	-3.38	-4.34	-5.16	-5.22

**Geometries.** The complexes Cp<sub>2</sub>Ti=PH, Cp(H<sub>3</sub>P)<sub>3</sub>V=PH, Cp(OC)<sub>3</sub>V=PH, Cp(H<sub>3</sub>P)Co=PH, and Cp(OC)Co=PH were investigated in addition to the already discussed Cp<sub>2</sub>Cr=PH and (OC)<sub>4</sub>Fe=PH. Geometrical parameters of the optimized structures are given in Table 2. The geometry of Cp<sub>2</sub>Ti=PH is in good agreement with data derived at the B3LYP/LANL2DZ level of theory.<sup>6</sup> The most relevant geometrical parameter for the present discussion is the M=P bond length. Using a shorthand representation, this is 2.352 (2.348)<sup>6</sup> Å for Ti=P, 2.286 Å for Cr=P, 2.326 and 2.307 Å for V=P, 2.192 Å for Fe=P, and 2.090 and 2.113 Å for Co=P. It appears that the M=P bond lengths decrease in the order Ti > V > Cr > Fe > Co, which corresponds exactly with the relative position of these transition metals in the periodic table. This suggests that the M=P bond length depends solely on the size of the transition metal. We note that the same metal size dependency appears to apply to the Cp–M distances, which are 2.042 and 2.055 Å for Cp–Ti, 1.993 and 1.980 Å for Cp–V, 1.834 and 1.845 Å for Cp–Cr, and 1.728 and 1.705 Å for Cp–Co.

**MO Interaction Diagrams.** Following the discussions on Cp<sub>2</sub>Cr=PH and (OC)<sub>4</sub>Fe=PH, it suffices here to focus on the energy levels of the singly occupied orbitals of the  $ML_n$  fragments in the geometry they possess in the complex. These are listed in Table 3 and make abundantly clear that the frontier orbital energies are directly related to the type and number of metal ligands (Cp > PH<sub>3</sub> > CO) rather than to the nature of the transition metal. The energy levels decrease gradually by replacing the Cp rings via PH<sub>3</sub> for CO ligands, and therefore, a smooth transition from nucleophilic Cp<sub>2</sub>M=PH (M = Ti, Cr) to electrophilic (OC)<sub>4</sub>Fe=PH can be expected. Illustrative are Cp(H<sub>3</sub>P)<sub>3</sub>V and Cp(OC)<sub>3</sub>V, which have the same transition metal but will differ in their philicity due to their different ligands.

**Atomic Charges.** The calculated charges on the phosphorus atom in the complexes are listed in Table 1 and are graphically displayed in Figure 2. They give the same decreasing order as the  $ML_n$  fragment orbital energies do, namely, Cp<sub>2</sub>Ti=PH > Cp<sub>2</sub>Cr=CH > Cp(H<sub>3</sub>P)<sub>3</sub>V=PH > Cp(H<sub>3</sub>P)V=PH > Cp(OC)Co=PH > Cp(OC)<sub>3</sub>V=PH > (OC)<sub>4</sub>Fe=PH. Thus, in accordance with the fragment MO energy analysis, the charges also emphasize the importance of the type of metal ligand on the philicity of the phosphinidene complex. Their values range from -0.270e for Cp<sub>2</sub>Ti=PH to -0.060e for the discussed (OC)<sub>4</sub>Fe=PH. We note that Frison et al.<sup>6</sup> also reported a concentration of charge on the phosphorus atom of Cp<sub>2</sub>Ti=PH in comparison to (OC)<sub>3</sub>Cr=PH.

**Bond Strengths.** The BDEs of the first-row transition metal phosphinidene complexes, listed in Table 4, show modest variations. They range from 39.1 kcal/mol for Cp<sub>2</sub>Cr=PH to

**Figure 2.** Calculated charges on the phosphorus atom of the first-row transition metal phosphinidene complexes  $ML_n=PH$ .

66.1 kcal/mol for Cp(H<sub>3</sub>P)Co=PH. Their  $\Delta E_{\pi}$  interaction energies are fairly constant (between -28.6 and -34.2 kcal/mol), while the differences are somewhat larger in the sizable  $\Delta E_{\sigma}$  (up to 18.5 kcal/mol) and still larger in the  $\Delta E^{\circ}$  components (up to 21.1 kcal/mol). The  $\pi$ -bond strength is in all cases about one-third (32–39%) of the  $\sigma$ -bond strength. It seems that the phosphinidene bond strength is relatively independent of the spectator ligands of the metal.

**Charge and Orbital Control.** The energy level of the LUMO of the phosphinidene complexes, which is the  $\pi^*$ -orbital<sup>28</sup> formed from an antibonding combination of the P( $p_x$ ) orbital and the metal  $d_{xz}$  orbital, depends on the amount of charge transferred from  $ML_n$  to the phosphorus and on the strength of the orbital interaction. Because the  $\pi$ -interaction is of the same order of magnitude for the entire series, this means that the position of the LUMO in the final complex is also predetermined by the relative energy of the fragment orbitals.

In fact, the orbital energy of the lowest unoccupied orbitals of the complexes increases with decreasing  $\pi$ -acceptor capability of the spectator ligands (Table 5) making an electrophilic attack on the phosphorus less likely. This trend is evident from the linear relationship ( $r^2 = 0.992$ ) of the LUMO orbital energies of the first-row phosphinidenes complexes with the corresponding P charges, as shown in Figure 3. Because charge control and orbital control work in the same direction, we are able to predict their philicity and thus the reactivity for these phosphinidene complexes.

**III. Ligand Variation for the Second- and Third-Row Transition Metal Groups.** In this section, we evaluate in a similar, but more condensed manner, the properties of those phosphinidene complexes that contain transition metals of the

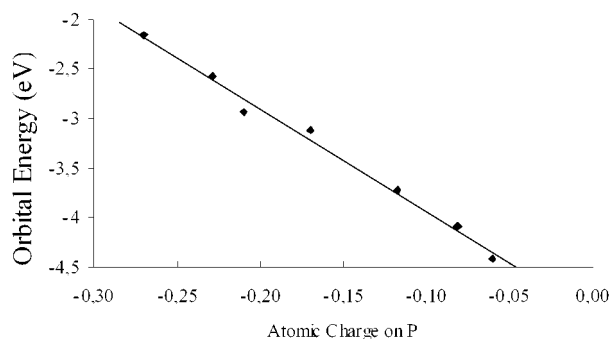
(28) In the case of the group IV complexes, the  $\pi^*$ -orbital is the LUMO + 1 due to the unfilled d shell of the transition metal.

**Table 4.** Bond Energy Analysis (in kcal/mol) for the Phosphinidene Complexes  $ML_n=PH$ 

	$Cp_2Ti=PH$	$Cp_2Cr=PH$	$Cp(PH_3)_3V=PH$	$Cp(PH_3)_3Co=PH$	$Cp(CO)_3Co=PH$	$Cp(CO)_3V=PH$	$(CO)_4Fe=PH$
$\Delta E_\sigma$	-91.0	-79.5	-98.0	-88.0	-85.4	-94.3	-90.7
$\Delta E_\pi$	-33.9	-30.0	-34.2	-27.9	-28.6	-37.2	-32.2
$\Delta E^\circ$	-10	-14	-10	6.0	8	2	11
$\Delta E^{tot}$	-74.4	-56.2	-67.0	-70.9	-70.5	-65.4	-67.6
BDE	60.0	39.1	49.5	66.1	65.8	52.8	61.7
	$Cp_2Zr=PH$	$Cp_2Mo=PH$	$Cp(PH_3)_3Nb=PH$	$Cp(PH_3)_3Rh=PH$	$Cp(CO)_3Rh=PH$	$Cp(CO)_3Nb=PH$	$(CO)_4Ru=PH$
$\Delta E_\sigma$	-100.7	-92.5	-101.6	-96.6	-93.9	-92.0	-91.2
$\Delta E_\pi$	-39.4	-35.7	-35.5	-32.7	-32.7	-34.1	-36.2
$\Delta E^\circ$	-6	5	-5	2	12	6	14
$\Delta E^{tot}$	-88.4	-76.8	-77.4	-81.0	-79.9	-70.9	-74.8
BDE	75.3	64.9	63.2	78.5	77.5	60.4	69.7
	$Cp_2Hf=PH$	$Cp_2W=PH$	$Cp(PH_3)_3Ta=PH$	$Cp(PH_3)_3Ir=PH$	$Cp(CO)_3Ir=PH$	$Cp(CO)_3Ta=PH$	$(CO)_4Os=PH$
$\Delta E_\sigma$	-105.2	-103.3	-110.9	-112.3	-108.0	-97.8	-98.5
$\Delta E_\pi$	-43.0	-39.5	-38.1	-39.1	-38.7	-35.5	-40.0
$\Delta E^\circ$	-8	0	-11	8	10	0	-1
$\Delta E^{tot}$	-98.3	-87.6	-83.3	-95.7	-93.6	-75.6	-83.4
BDE	80.7	75.6	68.1	92.4	90.7	68.1	77.1

**Table 5.** Calculated Energy Levels (eV) of the Lowest Lying Unoccupied Orbitals (LUMOs) of the Transition Metal Phosphinidene Complexes  $ML_n=PH$ 

$Cp_2Ti=PH$	$Cp_2Cr=PH$	$Cp(PH_3)_3V=PH$	$Cp(PH_3)_3Co=PH$	$Cp(CO)_3Co=PH$	$Cp(CO)_3V=PH$	$(CO)_4Fe=PH$
-2.16	-2.57	-2.93	-3.12	-3.72	-4.09	-4.41
$Cp_2Zr=PH$	$Cp_2Mo=PH$	$Cp(PH_3)_3Nb=PH$	$Cp(PH_3)_3Rh=PH$	$Cp(CO)_3Rh=PH$	$Cp(CO)_3Nb=PH$	$(CO)_4Ru=PH$
-1.86	-2.44	-2.83	-3.11	-3.70	-4.03	-4.00
$Cp_2Hf=PH$	$Cp_2W=PH$	$Cp(PH_3)_3Ta=PH$	$Cp(PH_3)_3Ir=PH$	$Cp(CO)_3Ir=PH$	$Cp(CO)_3Ta=PH$	$(CO)_4Os=PH$
-1.65	-2.25	-2.66	-2.78	-3.45	-3.96	-3.97

**Figure 3.** Dependency of the  $\pi^*$ -orbital energy of the first-row transition metal phosphinidene complexes on the atomic charge on phosphorus.

second and third rows. Relevant geometrical parameters, orbital energies, and atomic charges are summarized in Tables 2, 3, and 1, respectively, in addition to the data of the discussed systems with first-row transition metals.

Again, we see that, irrespective of the nature of the organometallic ligand (Cp or  $PH_3$  or CO), the  $M=P$  bond lengths follow the position of the transition metals in the periodic table. For the second row, this is Zr (2.473) > Nb (2.440, 2.441) > Mo (2.377) > Ru (2.317) > Rh (2.195, 2.203), with bond lengths (in Å) given in parentheses.

For the third row, the sequence is Hf (2.456) > Ta (2.436, 2.434) > W (2.379) > Os (2.337) > Ir (2.216, 2.210). The second-row  $M=P$  bonds are about the same length as those of the third row, and both are distinctly longer than the ones containing first-row transition metals.

In the case of the  $Cp_2M=PH$  ( $M = Mo, W$ ), the calculated structures compare very well with existing experimental data determined by X-ray crystallography for  $Cp_2M=PR$  ( $M = Mo, W$ ) with  $R = (2,4,6-t-Bu)_3C_6H_2$ .<sup>8,9</sup> The experimental  $Mo=P$  and

$W=P$  distances are 2.370(2) and 2.349(5) Å, respectively. The two  $Mo-Cp$  distances of 1.998 and 1.992 Å are also similar to those of the experimental  $Mo$  structure, i.e., 1.966 and 1.962 Å, as are the  $W-Cp$  distances (calculated, 1.981 and 1.980 Å; experimental, 1.98 and 1.93 Å). The theoretically predicted  $M-P-H$  angles of 103.6° ( $M = Mo$ ) and 103.1° ( $M = W$ ) are slightly smaller than the experimental ones (115.8(5)° and 125.8(2)°, respectively), reflecting the high steric hindrance of the  $(2,4,6-t-Bu)_3C_6H_2$  group.

The main distinguishing feature is again the charge on the phosphorus atom, which follows the same order as seen for the complexes containing first-row transition metals. Thus,  $Cp_2M=PH > Cp(H_3P)_3M=PH$  (Zr, Mo, Hf, W) >  $Cp(H_3P)_3M=PH$  (Nb, Ta) >  $Cp(OC)_3M=PH$  (Rh, Ir) >  $Cp(OC)_3M=PH$  (Nb, Ta) >  $(OC)_4M=PH$  (Ru, Os), where the metals  $M$  are given in parentheses. This differentiation comes about because of the different energy levels of the highest singly occupied  $a'$  and  $a''$  orbitals of the triplet  $ML_n$  fragment. The data of all first-, second-, and third row phosphinidene complexes in Tables 1 and 3 illustrate nicely the decrease in the  $ML_n$  orbital energy and in the charge on phosphorus on going from charge-donating to charge-accepting ligand systems.

The  $P=M$  bond dissociation energies (given in kcal/mol) do vary between the various types of phosphinidene complexes (Table 4), but they are remarkably similar for the most electrophilic and nucleophilic ones within each row, i.e.,  $Cp_2Ti=PH$  (60.0) and  $(OC)_4Fe=PH$  (61.7) for the first row,  $Cp_2Zr=PH$  (75.3) and  $(OC)_4Ru=PH$  (69.7) for the second row, and  $Cp_2Hf=PH$  (80.7) and  $(OC)_4Os=PH$  (77.1) for the third row. The most apparent systematic deviations are as follows: (1) the BDEs of the  $Cp_2M=PH$  complexes of group VI (Cr, Mo, W) are smaller than those of group IV (Ti, Zr, Hf), and (2) within each row, the complexes of group V (V, Nb, Ta) have



the smallest BDEs (except for  $\text{Cp}_2\text{Cr}=\text{PH}$ ), which appears to result from their larger  $\Delta E^\circ$  contribution. Throughout all phosphinidene complexes, the  $\pi$ -bond strength is slightly more than one-third of the  $\sigma$ -bond strength, i.e., 34–41% for both the second row and third row, and ranges from 32.7 to 43 kcal/mol. Even more striking is that, like the total BDEs, the  $\Delta E_\pi$  are also virtually identical for the most nucleophilic and electrophilic complexes within each row. Within each column of the periodic table, the BDEs of the third row phosphinidene complexes are larger than those of the second row, which are again larger than those of the first row.

The entries in Table 5 show that the orbital energy of the LUMO increases on going from the first- to the second- and third-row transition metals too, which is in line with the strength of the orbital interactions discussed above.

### Conclusions

The reactivity of phosphinidene complexes, stabilized by a transition metal group ( $\text{L}_n\text{M}=\text{P}-\text{R}$ ), has been rationalized by theoretical methods in terms of their philicity. The calculated partial charge on the phosphorus atom together with the energy level of the  $\pi^*$ -orbital determines a phosphinidene complex to be electrophilic or nucleophilic. This distinction depends on the metal moiety and can be influenced by its spectator ligands L.

The calculated geometries, which agree well with those known for Schrock-type complexes, show the length of the

metal–phosphorus bond for all studied complexes to depend solely on the atomic size of the transition metal and not on the nature of its ligands. This  $\text{M}=\text{P}$  bond, which can be described in terms of an interaction between triplet  $\text{ML}_n$  and triplet  $\text{PH}$ , has a strong  $\pi$ -component and an even stronger  $\sigma$ -component. This metal–phosphinidene interaction increases on going from the first- to the second- and third-row transition metals.

The chemical reactivity of experimentally yet unknown phosphinidene complexes can be predicted. Those that have a transition metal with strong  $\sigma$ -donor ligands, such as  $\text{Cp}^-$ , concentrate negative charge on the phosphorus atom and raise the energy of the  $\pi^*$ -orbital, thereby enhancing their nucleophilicity. Conversely, ligands with strong  $\pi$ -acceptor capabilities, such as CO, reduce the charge concentration on P and stabilize the  $\pi^*$ -orbital, both of which enhance the electrophilicity of the phosphinidene complex.

**Acknowledgment.** A.W.E. thanks the European Union for a Marie Curie postdoctoral fellowship. We thank The Netherlands Organization for Scientific Research (NCF/NWO) for providing a grant for supercomputer time.

**Supporting Information Available:** Cartesian coordinates of the optimized structures (PDF). This material is available free of charge via the Internet at <http://pubs.acs.org>.

JA017445N